Rheology-morphology relationships of new polymer-modified bitumen based on thermoplastic polyurethanes (TPU)

Raïssa Gallu, Françoise Méchin, Florent Dalmas, Jean-François Gérard, Rémi Perrin, Frédéric Loup

Rheology-morphology relationships of new polymer-modified bitumen based on thermoplastic polyurethanes (TPU).

Raïssa Gallu[1,2], Françoise Méchin[1], Florent Dalmas[2*], Jean-François Gérard[1], Rémi Perrin[3], Frédéric Loup[4]*

[1]Univ Lyon, INSA Lyon, CNRS, UMR 5223 IMP, F-69621, Villeurbanne, France.
[2]Univ Lyon, INSA Lyon, CNRS, MATEIS, UMR 5510, F-69621, Villeurbanne, France.
[3]Soprema Co., 14 rue Saint Nazaire, 67100 Strasbourg, France.
[4] Eiffage Infrastructure, Corbas, France.

Keywords: polymer-modified bitumen; thermoplastic polyurethane; morphology; phase separation; mechanical behavior

ABSTRACT:

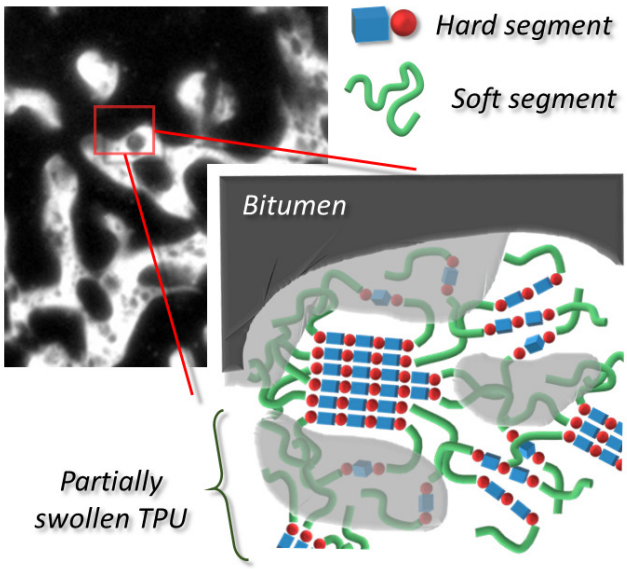

The present study reports a new type of polymer-modified bitumen (PMB) which considers the use of a thermoplastic polyurethane (TPU) as an alternative to conventional thermoplastic elastomers such as poly(styrene-b-butadiene-b-styrene) block copolymers. As for other block copolymers, the structure of the TPU, made of two types of segments

which can microphase-separate, leads to its selective swelling by the oily fractions of bitumen. The poor compatibility of hard segments (HS) with bitumen is responsible for this partial swelling of the TPU by the maltene fractions. By varying the TPU content in the bitumen-TPU blend a dramatic change in viscoelastic properties for a TPU content close to 11wt% is shown, with the appearance at high temperatures of an elastic response due to the percolation of the TPU-rich phase. This percolation phenomenon is highlighted by multiscale morphology characterizations and well described by a conventional mechanical percolation model. Different TPU architectures, i.e. different hard to soft segments ratios, are studied. The best compromise is found for a blend containing TPU with 13 wt% of HS as it displays a favorable swelling of percolated TPU rich phase while maintaining its viscoelastic behavior.

INTRODUCTION. Bitumen are well known for their applications in road pavement and roofing. Many papers described bitumen composition and rheological properties, which are of first importance since these applications namely require a good plasticity at low temperatures, a good creep resistance at high temperatures, as well as a high flow temperature. The chemical composition of bitumen is usually described by four main species denoted as SARA fractions, i.e. saturates, aromatics, resins, and asphaltenes[1–3]. These four fractions differ in polarity and molar mass, with saturates being the less polar and having the lowest molar masses. On another hand, the resins and asphaltenes are the most polar fractions with the highest molar masses[3,4]. Asphaltenes are defined as non-soluble in heptane[4,5] where they precipitate and lead to a black powder. The other three fractions (saturates,

aromatics, and resins) form the oily fraction, well known as the maltenes fraction. Chromatography techniques help to give average weight contents of the four SARA fractions in bitumen[6,7].

Bitumen is also often presented as a colloidal structure, where the resins interact with asphaltenes to ensure their dispersion in the oily fractions[3,8]. As a consequence, bitumen structure is strongly dependent on the content of dispersed asphaltenes particles in the maltenes fraction. As a consequence, based on the colloidal model, one can explain the dependence of the rheological properties of a bitumen with its chemical composition[9–13]. Bitumens display a Newtonian behavior at high temperature, with a viscosity controlled by the SARA fractions contents. Thus, the highest viscosities are observed with high asphaltene and low aromatic contents[14]. Mechanical properties of bitumen also depend on the temperature. At very low temperature, bitumen becomes brittle, and the road pavement no longer meets the mechanical resistance requirements leading to cracking in the material, whereas at high temperature, rutting occurs[15]. To prevent cracking at low temperature and rutting at high temperature, bitumen can be modified by polymers or additives such as acids and low molar mass compounds[16,17], or a combination of both[18–24]. The polymer phase could swell with low molar masses fractions in order to stop crack propagation (at low temperatures) and increase the glass transition (T_g) of the bitumen phase (improvement of the creep behavior in the high temperatures region).

The most used polymers to modify bitumen are polyolefins and thermoplastic elastomers (TPE)[25,26]. In the last decades was reported the modification of bitumen with the TPE

styrene-b-butadiene-b-styrene (SBS) block copolymers which found industrial applications in road pavements. SBS block copolymers display a microstructure combining a soft polybutadiene phase with rigid polystyrene nanodomains[27]. Linear SBS block copolymers are the most used in bitumen modification, due to partial compatibility of the polymer with bitumen SARA fractions, as shown with the incomplete overlapping of the solubility spheres of both SBS and bitumen when using the three dimensional Hansen solubility parameters[28]. Bitumen presents a preferential compatibility with the polybutadiene soft block, which is illustrated by a decrease in swelling and dispersion of the polymer in the blends when the styrene content increases[29,30]. This partial compatibility gives rise to partial swelling of the SBS block copolymer by some of the bitumen low molar mass fractions, leading to a partial depletion of the bitumen phase and consequently to an increase of its T_g and modulus.

SBS modified bitumen are biphasic materials whose morphology is usually characterized by fluorescence microscopy, where the polymer-rich phase fluoresce within the dark bitumen asphaltene-rich phase because of its swelling by aromatic compounds[31]. The resulting morphology as well as the viscoelastic properties of blends depend on the amount of added polymer but also on several parameters regarding the SBS block copolymer, such as its macromolecular architecture, its nature, i.e. linear or star-like, the styrene:butadiene ratio, etc.[29,30,32,33]. For linear SBS block copolymers, with a styrene content of 31 wt%, a bitumen modified with 3 wt% of polymer shows a morphology with a dispersed polymer rich phase, while at contents higher than 6 wt% a continuous SBS rich phase appears[33]. Lu and

Isacsson[33] reported that the mechanical behavior of a bitumen-polymer blend remains asphalt-like at low polymer content, up to the appearance of the continuous polymer rich phase, highlighted by a change in the viscoelastic properties toward a polymer-like behavior. In this last case, it appears that this continuous swollen polymer phase is mainly responsible for the mechanical response of the blends. After T_g, sometimes well-above Tg (close to room temperature, hence more than 40°C above Tg, as shown in reference [33] for instance) depending on SBS content, SBS-modified bitumen shows a higher modulus compared to neat bitumen, due to the presence of incompatible mechanically active styrene hard domains, and at high SBS content, a lower modulus before T_g, as the continuous SBS-rich phase governs the mechanical properties[34].

As a consequence, cracking resistance is improved due to the increase in the elasticity of the bituminous material resulting from the swelling of the polymer by the maltenes, leaving the asphaltenes apart[35,36]. Similar works have been done for other types of copolymers, such as poly(ethylene-co-vinyl acetate) (EVA)[37–39].

The current work reports the modification of a bitumen with thermoplastic polyurethanes, which has been very scarcely described in literature in the last years. Nevertheless, some works can be found in the recent literature dealing with the modification of bitumen with TPU in physical blends for roofing applications[40] or road pavements[41,42]. Polyurethane has also been used in other studies as a reactive polymer to modify bitumen either for processing bituminous foams or to create chemical reactions inducing covalent bonds between the polymer and bitumen's species in order to prevent phase separation in the

corresponding blends[43–49]. The versatility of the structure of TPU is of great interest since it can be tailored to meet any specific application requirements. Indeed, TPU is basically composed of three components: a high molar mass polyol, a diisocyanate, and a chain extender such as a low molar mass diol[50–52]. The chemical structure of these three components can be changed to give rise to a large range of TPU with tailored mechanical properties and/or thermodynamic affinities. The reaction of the diisocyanate with the polyol leads to the formation of soft segments, denoted SS and having T_g lower than room temperature, while the reaction of the diisocyanate with the short diol leads to the formation of hard segments, denoted HS having a T_g above room temperature. As for SBS, TPU usually display a nanoscale morphology with two phases: a hard segment-rich dispersed nanophase and a soft segment-rich continuous phase. As a consequence, the composition and molar mass of TPU can be adjusted to reach the desired microstructures and mechanical properties, since the phases can be either amorphous or semi-crystalline depending on the nature of the components used.

This paper deals with a reference bitumen modified with different amounts of TPU having various compositions, namely various HS contents. The study aims to describe the rheological behavior of the resulting bituminous materials regarding their morphology at different scales.

EXPERIMENTAL SECTION

Materials. A bitumen having a penetration grade (ASTM D5) of 160/220 was used as the reference material to prepare bitumen-polymer blends. This bitumen shows penetration of 176 10^{-4}m and a Ring and Ball (R&B) softening point (ASTM D36) of 43°C. The composition in terms of SARA fractions of the bitumen based on liquid chromatography test gives a content of 10 wt% for saturates, 62 wt% for aromatics, 15.5 wt% for resins and 12.5 wt% for asphaltenes. A thermoplastic polyurethane from Soprema Co., referred as TPU13 was used as the reference polymer for modification. This polymer was synthesized by reactive extrusion from a polyester polyol based on fatty acid named as Radia 7285, 4,4'-methylene bis(phenyl isocyanate) (MDI), and 1,4-butanediol (BDO) as chain extender. This reference TPU contains 13 wt% MDI-BDO hard segments.

Other polymers were synthesized with a similar chemical composition but varying amounts of MDI-BDO hard segments. MDI and BDO were provided by Sigma Aldrich Co., and the polyester polyol Radia 7285 was provided by Oleon Co and known to have a hydroxyl number of 35.8 mg KOH.g^{-1}.

Methods. TPU with different HS contents ranging from 8 to 30 wt%, were synthesized using a two-step procedure involving the formation of a polyurethane prepolymer as intermediate[51,52]. In the first step, the procedure consisted in adding the polyester polyol and a variable excess of MDI diisocyanate in a 300 mL closed reactor at 80°C. The mixture was placed under nitrogen atmosphere and stirred at 600 rpm for 50 minutes. The precise required amount of chain extender BDO was then added in the reactor with a syringe and the mixture stirred at 1,000 rpm during 1 minute, then at 600 rpm for about 10 minutes according

to the viscosity changes. If the mixture became too viscous before the end of this stirring time, stirring was stopped and the polymer was poured on a metallic plate in an oven at 80°C for 12h to pursue the polymerization reaction. The polymer was then put between two metallic plates under a hot press at 110°C under 40 bar pressure for 1 hour and cooled to room temperature to process 2 mm thick TPU film.

To make the bitumen-TPU blends, 100 g of 160/220 grade bitumen were placed in a metal pot and heated at 180°C for 1h. Granules of TPU were added in the hot bitumen. Once the TPU was softened in the bitumen (30 minutes to 1 hour, depending on the HS content), the mixture was stirred at 2 500 rpm at 170°C for 15 minutes with a Rayneri agitator. The hot blend was poured on a silicon sheet which was placed between two metallic plates and pressed to obtain 2 mm-thick films that were then cooled down under ambient air to room temperature.

Instrumentation. Dynamic mechanical analysis (DMA) is made in torsion mode on a homemade pendulum, under inert atmosphere (helium) at 600 mbar between -120 and 130°C with a heating rate of 1 $K.min^{-1}$. The test is realized at constant frequency of 1Hz on samples of 2 mm thickness, width of 6 mm and length of 12 mm. Liquid nitrogen is used as cooling system.

Rheological properties of TPU are analyzed on an ARES device from TA instruments, at 1Hz between 20°C and 130°C with a plate-plate geometry of 25 mm of diameter, 2 mm gap and 2% strain.

Fluorescence microscopy tests were conducted using an optical microscope Zeiss equipped with a high pressure mercury UV lamp HBO in reflection mode with a two-filter system allowing to analyze specimens under 300-400 nm and 450-490 nm wavelength ranges. The polymer-modified bitumen samples were broken at low temperature in liquid nitrogen to allow analysis of the morphologies across the sample thickness. The fluorescence images obtained were segmented using the Fiji[53] software. The percentage of swollen TPU, which appears white in the images (due to the absorption of aromatic compounds), was then measured and averaged on at least five images. A swelling coefficient was then estimated as the ratio between the average surface fraction of TPU-rich phase measured in the images and the initial weight fraction of added polymer. Considering the close density values of bitumen and TPU, this coefficient is expected to be equal to one for non-swollen TPU and >1 when swelling occurs.

Samples for transmission electron microscopy were prepared by cryo-ultramicrotomy at -80°C using a UC7 Leica microtome device equipped with two diamond knifes, i.e. the first one for the pyramid preparation and the second one for cutting 100 nm thick-slices. TEM observations were conducted using a Philips CM120 with an acceleration voltage of 120kV at room temperature for the polymer and at -180°C for bitumen without any prior staining step.

Scanning electron microscopy (SEM) analyses were made using a Zeiss SUPRA55VP microscope with an acceleration voltage of 0.8 kV in secondary electron mode. Samples for SEM were first broken in liquid nitrogen and put for seven days in heptane at room

temperature to remove the oily bitumen fractions, since asphaltenes are not soluble in heptane.

Atomic force microscopy (AFM) was performed using a Dimension 3100 AFM device connected to a Nanoscope V scanning probe controller (from VEECO Instruments Co.). All images were obtained at room temperature in tapping mode using a pointprobe-plus® silicon (PPP-NCH-50) from Nanosensors Co. with a high resonance frequency (ca. 300 kHz). A lateral resolution of 3-5 nm can be achieved by this configuration with a vertical resolution of 0.5 nm. Very flat surfaces were obtained by cryo-ultramicrotomy. For this reason, only phase images (highlighting a hard/soft contrast) after treatment with Gwyddion freeware[54] are shown in the present paper.

RESULTS AND DISCUSSIONS

Bitumen properties. The neat bitumen was observed by cryo-TEM (Figure 1(a)) and a colloid-like microstructure was highlighted with three main components. First, the continuous phase can be attributed to the aromatic phases that constitute the major fraction in bitumen. Then the dispersed nano-droplets with size ranging from 0.1 to 1 µm may result from a phase separation of other incompatible molecules (resins and/or saturates). Finally, Figure 1(a) also shows a third phase in the bitumen that consists in darker elongated objects which are similar to stacks of layered structures. From the literature such compounds can be associated in bitumen either to crystalline waxy structures [55] or asphaltenes [56][57,58]. It is not clear from Figure 1(a) what such structures correspond to.

Such a microstructure is consistent with a sol-type bitumen state since no compact structures are involved. Differential scanning calorimetry (DSC) analyses (Figure 1(b)) of the neat bitumen evidence a glass transition temperature close to -40°C attributed to the major aromatic fraction, followed by several endotherms associated with the crystallization and melting phenomena of the saturates, high molar mass resins, and asphaltenes. These thermal properties are well described in literature by Masson et al[59].

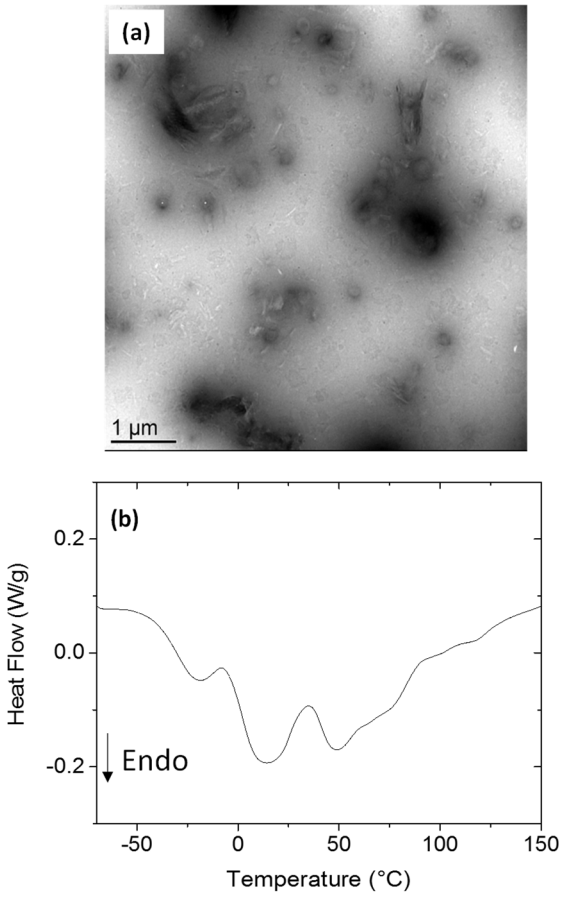

Figure 1. a) TEM micrograph of the neat bitumen observed at -170°C without any chemical staining; b) DSC trace of the neat bitumen.

Thermomechanical behavior of neat TPU. Figure 2 displays combined isochronal DMA (solid state) and rheology curves measured at 1Hz for all the TPU with various HS contents.

At low temperature, all the TPU display almost the same modulus. The main relaxation (associated with the glass transition) occurs for all TPU at -54°C, denoting the existence of a well-separated soft phase with a rather constant composition. Above this temperature, and for HS contents higher than 8 wt%, TPU behave like thermoplastic elastomers as a rubbery plateau is evidenced, followed by their rubbery flow at high temperatures after melting of pseudo-crystallized hard segments, i.e. above 170°C (See DSC results in Figure S1 in supporting information revealing endothermal peaks in TPU with high HS contents). This thermoplastic elastomer behavior results from the presence of the mechanically effective crosslinks formed by the association of hard segments as nanodomains. For 8 wt% of HS, the TPU does not contain enough associated HS units in nanodomains to display a rubbery plateau before HS softening. As a consequence, 8 wt% HS-based TPU behaves like an amorphous thermoplastic. As shown in Figure 2, large changes of the storage modulus could be evidenced by changing the HS content. Increasing the HS content of the TPU from 13 to 30 wt% leads to an increase in the storage modulus in the rubbery state (from 1 MPa to 5 MPa at 50 °C, respectively).

The presence of nanodomains of associated hard segments, acting as reinforcing fillers, in TPU explains the increase of the modulus at the rubbery plateau as the hard segment content increases (see TEM images and SAXS profiles obtained for all TPU in Figure S2 and S3 respectively in SI, published in a separated article[60]). Similar results have been reported in the literature for TPU with closely-related chemical structures[61].

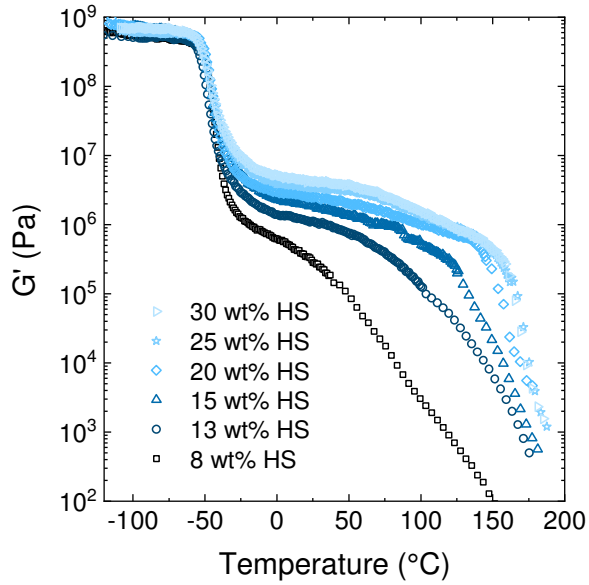

Figure 2. Storage shear modulus, G', as a function of temperature at 1 Hz of TPU synthesized according to a two-step procedure and containing different amounts of MDI/BDO hard segment.

Polymer (TPU13)-modified bitumen. Fluorescence microscopy investigations of the blends as a function of TPU content (Figure 3) show, as expected, that the polymer-modified bitumens are two-phase materials. The TPU-rich phase appears as the fluorescent phase (in white) due to the swelling by fluorescent aromatic compounds, whereas the bitumen-rich phase remains dark on the reported micrographs. For low TPU contents, a micrometric polymer-rich phase dispersed in a continuous bituminous phase is highlighted. For 17 wt% of TPU a phase inversion is observed, i.e. a morphology with co-continuous networks of polymer and bitumen. Then, a continuous TPU phase appears with dispersed bitumen-rich domains (with smaller diameters of the order of 10 µm) with increasing TPU content. From fluorescence microscopy micrographs, average swelling coefficients were estimated with

values comprised between 1.5 and 1.8 for blends containing between 9 and 17 wt% TPU, meaning that the TPU is obviously swollen by some fractions of the bitumen.

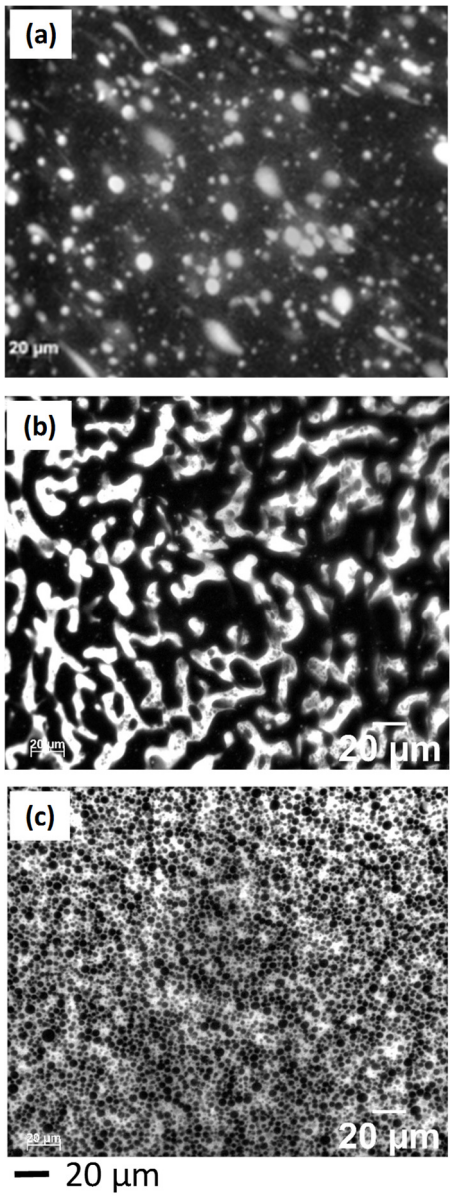

Figure 3. Fluorescence microscopy micrographs of TPU13 (in white)-bitumen (in black) blends: (a) 9wt% TPU13; (b) 17wt% TPU13; (c) 30wt% TPU13 (scale bar is the same for all 3 images).

Further investigations of the morphology were made by electron microscopies and AFM (Figure 4). Scanning electron microscopy (SEM) of a TPU/bitumen blend containing 30 wt% TPU after removal of the heptane-soluble fractions (i.e. maltenes, since the TPU is not soluble in heptane) confirms the morphology observed using fluorescence microscopy (Figure 4(a)) consisting in spherical domains of bitumen-rich phase with a diameter of a few micrometers dispersed in a continuous polymer phase. Similar correlations could be done for 17 wt% of TPU (see Figure S4 in SI where SEM observations show the continuous TPU network after heptane treatment).

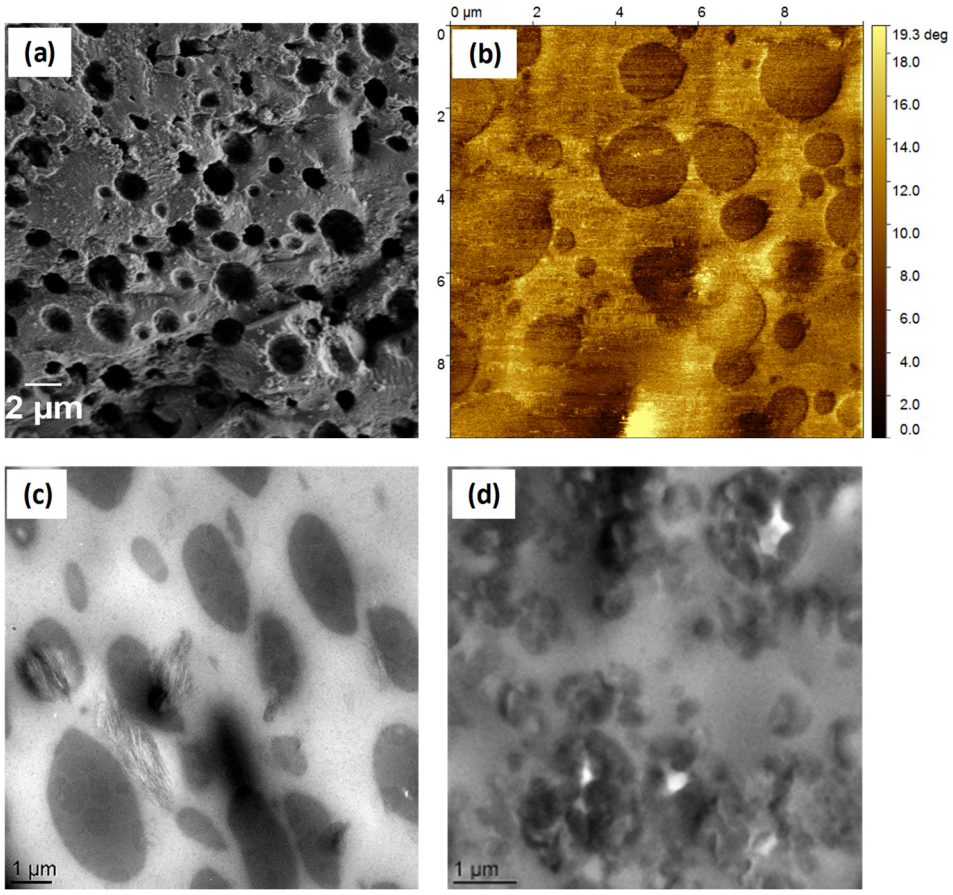

Figure 4. Morphology of the bitumen-TPU blend for 30wt% TPU13 content. (a) SEM image after solvent (heptane) treatment; (b) AFM phase image of the untreated blend (increasing

phase angle = increasing hardness); (c) TEM image of the untreated blend; (d) TEM image after solvent treatment (heptane).

Investigations at smaller length scales using TEM and AFM microscopies of the 30 wt% TPU13-bitumen blend are shown in Figure 4(b)-(c) and confirm the optical microscopy observations while revealing smaller bitumen domains. It is important to note that the elongated shape of the bituminous phase appearing in dark in TEM images is an artefact coming from the cryo-microtomy procedure. These domains can therefore rightly be associated to the circular domains observed by AFM and SEM. Such a multi-scale morphology was also observed by TEM on SBS-modified bitumen[62]. AFM phase contrast images (Figure 4(b)) show that the dispersed bitumen phase is softer than the swollen TPU-rich continuous phase (darker contrast). TEM images also show dispersed micron-size layered aggregates (Figure 4(c)). Some researchers reported a graphene-like layered structure for asphaltenes by TEM[57,58] which is consistent with such structures observed in this work.

Another conclusion could be made regarding the composition of the dispersed bitumen phase in the blends. Considering TEM observation of the blend after heptane extraction in Figure 4(d), dark objects are still observable within the polymer phase and correspond to asphaltene particles since heptane dissolves maltene phases, as previously mentioned. These asphaltenes particles show a globular morphology, as also observed in [56], highly different from the previously observed lamellar assemblies within the blend before extraction.

From the previous multi-scale microstructural characterizations, we can then conclude that in TPU-bitumen blends most of the maltene oil fraction swells the polymer phase. The remaining insoluble bitumen phase is then segregated in spherical micro and nanodomains highly concentrated in asphaltenes.

Rheological behavior of TPU-modified bitumens. Rheological curves, i.e. shear storage modulus, G', as a function of temperature, of bitumens modified with TPU13 are shown in

Figure 5. By changing TPU content from 0 to 30 wt% in the blends, a change in the rheological response can be clearly evidenced between 9 and 11 wt% of TPU. In fact, the blend with 9 wt% of TPU flows just above bitumen's T_g and has the same viscous behavior as bitumen, whereas for higher TPU contents, a rubbery-like plateau is evidenced (supported by a loss factor, tan δ, lower than 1 in this temperature range, see Figure S5 in SI). This means that the TPU-bitumen blend behaves like an elastomer for a given range of temperature before flowing, typical behavior of a thermoplastic elastomer (TPE). This behavior is evidenced by a high increase of Ring and Ball (R&B) softening point between 9 and 13 wt% TPU (see Table S1 in SI). It could be emphasized that the plateau modulus increases as the TPU13 content increases. At higher temperature, all blends modified with large amounts of TPU flow at the same temperature, i.e. after relaxation of the MDI/BDO hard segments occurring close to 107°C[63]. These observation are in full agreement with previous microstructural characterizations. For TPU contents higher than 9-11 wt%, a phase inversion occurs in the blends resulting in a bitumen-rich phase dispersed in a swollen polymer-rich continuous phase. Rheological properties of the blends are then driven by the behavior of this swollen

TPU continuous phase. A TPE-like behavior is observed in a temperature range above T_g of bitumen and TPU, meaning that HS nanodomains are maintained in the TPU even after swelling by maltene fractions. These observations suggest that the maltenes selectively swell the soft segments-rich phase of the TPU, leaving the hard segments-rich phase unswollen. This phenomenon is well-known in polymer-modified bitumen systems as "partial swelling" and the polymer content at phase inversion depends on the nature of both constituents. As an example, for SBS- or polyethylene-modified bitumens, only the butadiene block or the amorphous phase, respectively, are swollen by the maltenes and the phase inversion occurs for only 6 wt% of polymer[33,35],[64].

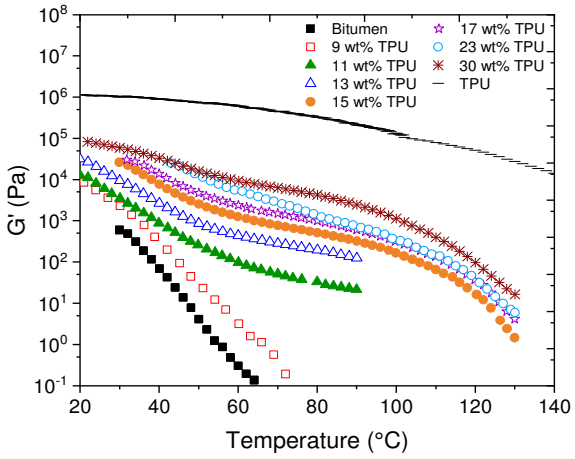

Figure 5. Rheological properties at 1 Hz of a bitumen modified with TPU13. Shear storage modulus of blends containing different TPU contents as a function of temperature.

As previously discussed, the phase inversion phenomenon can be described as the percolation of the TPU rich-phase for blends based on more than 10 wt% of TPU. As a consequence, the blends display a thermoplastic elastomer behavior whereas the bitumen phase made of

asphaltene and residual maltene fractions has a viscous behavior. Above the TPU content required for phase inversion, the thermomechanical properties of the blends are driven by those of the swollen TPU continuous phase and all blends with TPU contents higher than 13 wt% flow at the same temperature.

To support this hypothesis, a description of the mechanical storage modulus of TPU13-bitumen blends is proposed based on a series-parallel model and a percolation concept[65–67] (Eq. 1-3). Considering a random distribution of rigid phase denoted r, e.g. the swollen TPU-rich phase, in an infinitely soft matrix of bitumen, the percolation theory gives a volume fraction P of percolating phase. P can be expressed from the percolating threshold Φ_c and an empirical critical exponent b approximated to 1.8 according to De Gennes' theory[68]. The volume fraction can be expressed by the following equation:

$$P(\Phi) = 0, \ \Phi < \Phi_c \qquad \text{(Eq. 1)}$$

$$P(\Phi) = \left(\frac{\Phi - \Phi_c}{1 - \Phi_c}\right)^b, \Phi \geq \Phi_c \qquad \text{(Eq. 2)}$$

The model describes the association of the rigid phase of swollen TPU in parallel with a bitumen matrix and some non-percolating TPU rich phase. Thus, the storage modulus G' of the blend is given by:

$$G' = \frac{(1 - 2P(\Phi) + P(\Phi)\Phi)G'_m G'_r + (1 - \Phi)P(\Phi)G'^2_r}{(1 - \Phi)G'_r + \big(\Phi - P(\Phi)\big)G'_m} \qquad \text{(Eq. 3)}$$

with G'_m and G'_r the storage moduli of the bitumen matrix and the swollen TPU, respectively.

Figure 6 shows the evolution of G' as a function of the TPU content in blends. A good fit between experimental and calculated values is found with a percolation threshold Φ_c equal to 10 ± 1 wt%, b equal to 2.1 ± 0.1 as a critical exponent, and a modulus for the percolating phase G'_r of 0.07 MPa. Considering the complexity of such a multiphase system, it could be assumed first, that the swelling ratio of the polymer-rich phase is similar whatever the TPU content and, secondly, that this swollen TPU maintains its thermoplastic elastomer character ensuring a constant storage modulus in the rubbery state of the percolating phase. Thus, as previously mentioned, this latter conclusion means that in partially swollen TPU phase, HS domains remain associated to ensure physical crosslinks in the TPU. A two-dimensional swollen coefficient was previously estimated to 2 for this TPU by image analysis. Considering the classical theory for rubber elasticity in elastomer network (see [69] for instance), if a crosslinked polymer is swollen with a solvent, the number of chains occupying a given volume has decreased and the polymer Young's modulus is decreased by $\nu^{1/3}$ where ν is the volume fraction of polymer in the swollen material, i.e. the inverse of the volume swollen coefficient. Here the 3D swelling coefficient can be estimated to $2^{3/2}$. Thus, the Young's modulus should be divided by a factor of $2^{1/2}$~1.41, much lower than the value of 8 found by considering the neat TPU modulus (around 0.5 MPa in Figure 2) and the "percolating phase" modulus, G'_r, adjusted to 0.07 MPa. As a consequence, the only swelling of the soft phase of the TPU by the maltene fraction cannot explain the observed softening, which is therefore also linked to a modification of the elastically active network, i.e. here to the rigid nanodomains of HS playing the role of physical cross-linking nodes.

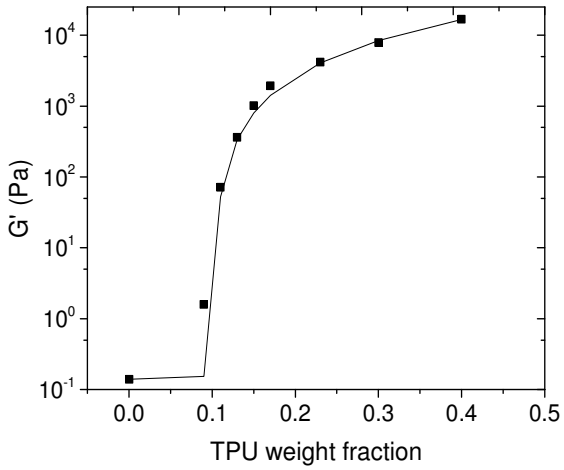

Figure 6. Experimental storage modulus at 64°C of the TPU-bitumen blends as a function of the TPU content (dots); calculated values of the storage modulus using a percolation model (solid line).

Influence of TPU composition. The influence of TPU composition on the properties of the TPU-bitumen blends was studied by varying the amount of hard segments MDI/BDO in the TPU in blends containing a constant amount of 15 wt% of TPU. Figure 7 shows the morphology of these blends observed by fluorescence microscopy. At low HS contents, a continuous TPU-rich phase with a dispersed or co-continuous bitumen phase is observed, whereas at high HS contents, only dispersed domains of TPU-rich phase are present. To go further, an estimation of the swelling coefficient of the TPU in the blend regarding its HS content is made from image analysis (Figure 8). A neat decrease in this coefficient is observed when the HS content increases. As plotted in Figure 8, it is assumed that MDI/BDO HS are not swollen by bitumen SARA fractions, i.e. the soft segments are mainly concerned for the

swelling of the TPU in bitumen. This suggests that soft segments prepared with Radia 7285 and MDI display a good compatibility with bitumen, whereas the HS do not.

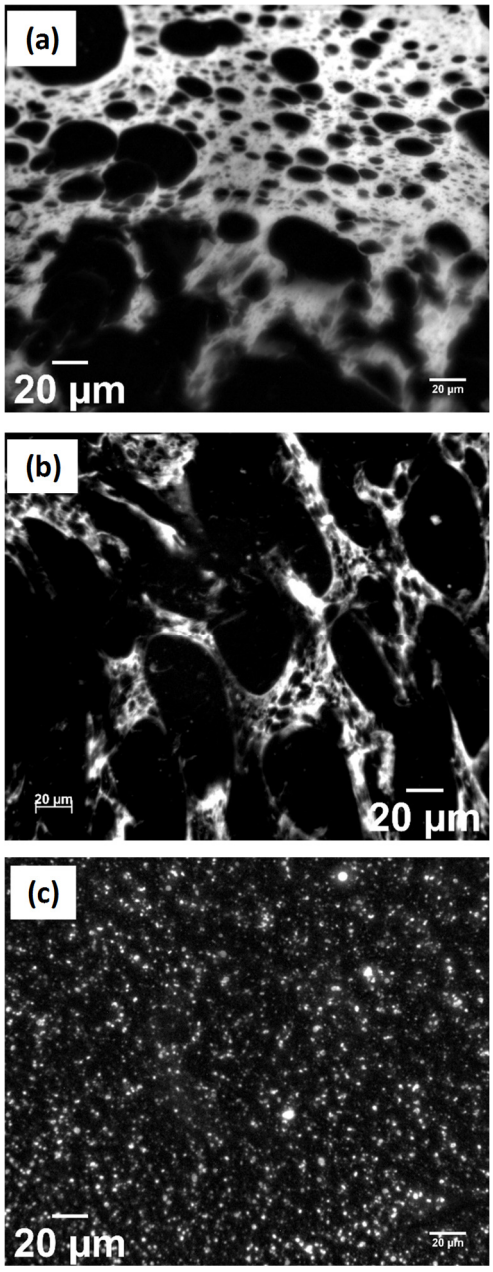

Figure 7. Fluorescence microscopy images of bitumen-TPU blends containing 15wt% TPU with various hard segment (HS) contents: (a) 8wt% HS; (b) 13wt% HS; (c) 30wt% HS. Bitumen and TPU appear in black and in white, respectively.

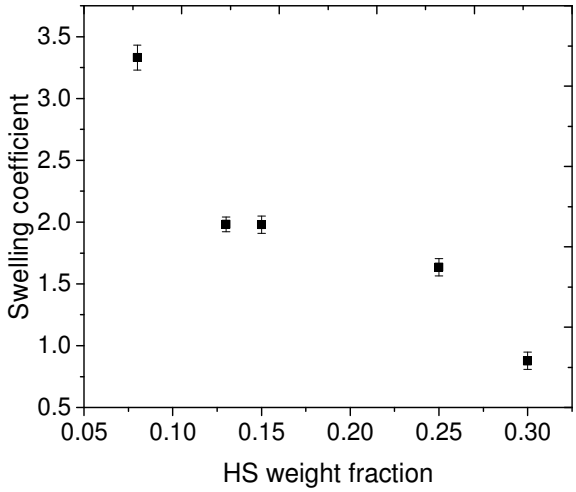

Figure 8. Swelling coefficient of TPU in the 15 wt% TPU-bitumen blends as a function of the hard segments content.

Thus, it should be emphasized as previously shown, that the morphology of the blends depends on the TPU content as well as on its chemical structure.

For SBS-modified bitumen, several studies have also reported a change of the morphology of blends when varying the hard styrene block content in the polymer. In fact, for most cases, a higher swelling of the SBS is noticed as the polystyrene content is low[29,30], which is relevant with this study.

Rheological properties of the corresponding blends were studied (see

Figure 9). Three distinct behaviors are observed: i/ an increase in the storage modulus with preservation of the viscous flow above T_g of the bitumen for the blends based on TPU having from 8 to 11 wt% of HS; ii/ the appearance of a rubbery plateau (i.e; G' almost constant with temperature and tan $\delta < 1$ on Figure S6 in SI) above T_g of the bitumen for blends based on

TPU having from 13 to 25 wt% of HS conferring a TPE mechanical behavior to the TPU-bitumen blends; iii/ for a blend based on a TPU having 30 wt% of HS, the rubbery plateau disappears, meaning that the blend behaves again as a viscous medium above the T_g of the bitumen. In addition, increasing HS content above 13 wt% HS leads to a decrease of the storage modulus at the rubbery plateau from 10^3 to 10^2 Pa. Regarding the morphology presented before, it can be concluded that the presence of a continuous TPU-rich phase isn't a sufficient condition to impart a TPE behavior to the TPU-bitumen blends.

For the neat TPU, we have previously shown an increase in the storage modulus at the rubbery plateau as the HS content increases (Figure 2). In addition, the TPU morphology becomes more complex at high HS contents considering the semi-crystalline nature of HS separated phase (see SI microstructural analyses in Figure S7). It is then necessary to consider the interactions of the various bitumen fractions with hard and soft phases individually. As reported previously, as the swollen TPU phase governs the mechanical properties from the phase inversion phenomenon, the occurrence of the rubbery plateau when increasing the HS content suggests that this continuous (or percolating) polymer phase behaves as a thermoplastic elastomer at high temperature. Such a behavior can be achieved in TPU thanks to HS associations within nanodomains acting both as physical crosslinks and reinforcing objects within the continuous TPU-rich phase, as evidenced by the high storage modulus in the rubbery state and the delayed flow temperature. Indeed, the flow temperature of the blends increases for TPU having between 11 and 13 wt% of HS and remains constant for TPU having more than 13 wt% HS. This phenomenon is related to the HS domains that are

prone to flow above 107°C at the most if amorphous, but only above 150-200°C if they are semi-crystalline. Those last observations for HS content between 8 and 15 wt% highlight the partial swelling of the TPU by the oil or maltene fractions of the bitumen. Indeed, while the soft phase is swollen by oil, hard segments appear incompatible with bitumen and their domains are maintained in the TPU phase conferring elasticity at high temperature (see illustration in Figure 10).

A further increase in the HS amount induces a detrimental decrease in the swelling of the TPU phase (Figure 8), the loss of the continuity of the TPU-rich phase (Figure 7) and, consequently, the loss of the elastomeric behavior of the blend at high temperatures.

It should be noticed that the optimal hard segments/soft segments ratio of the TPU polymer would depend on the polymer architecture and segment chemical nature, and consequently different TPU would probably lead to different optimal hard segments/soft segments ratios.

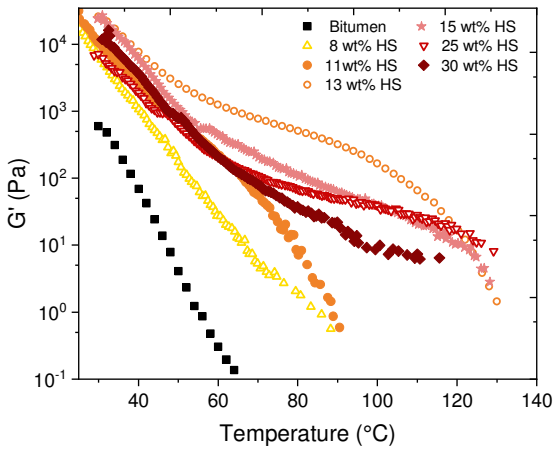

Figure 9. Rheological properties of bitumens modified with 15 wt% of TPU at 1 Hz. Storage modulus, G', of blends containing TPUs having different HS contents as a function of temperature.

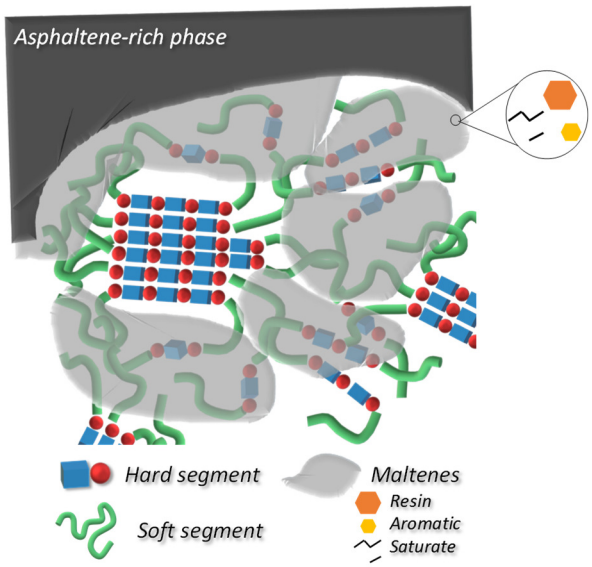

Figure 10. Schematic representation of the swelling of the TPU in bitumen.

CONCLUSION. The present work highlights the challenge for designing the most appropriate thermoplastic polyurethane to modify a given bitumen. Indeed, regarding the requirements for having high performance bituminous materials, a compromise should be made between good compatibility and mechanical properties, which are mainly achieved by tuning the polymer architecture. Two factors should be taken into account: i/ the TPU content in the blend associated with a good compatibility with bitumen that should be high enough to induce TPU swelling and phase inversion, i.e. percolation of the TPU-rich phase, within the blends and, ii/ the amount of HS (that have to be incompatible with bitumen) in this

swollen TPU phase, which then drives the thermo-mechanical behavior of the blend, should be higher than a critical value (found here around 13 wt%) in order to maintain an elastomeric behavior of the TPU-rich phase in a temperature range between the soft phase glass transition and the HS melting point.

It is therefore quite clear that the partial swelling of the TPU by the different SARA fractions of the bitumen plays an essential role in the optimization of the mechanical behavior of the blends. In order to better understand this phenomenon and to find the best compromise more efficiently in TPU-bitumen blends, further investigations on compatibility between the two types of segments of the TPU and SARA fractions of bitumen will be discussed in another study.

ASSOCIATED CONTENT

Supporting information. Figure S 1. Differential scanning calorimetry traces of TPU having various MDI/BDO hard segment contents and of the pure MDI/BDO hard segment.

Figure S 2. TEM images of TPU containing MDI/BDO hard segments: a) 13wt% HS; b) 15wt% HS.

Figure S 3. SAXS patterns of TPU varying from their HS content c) 30wt% HS.

Figure S 4. SEM image of blend containing 17wt% TPU13 after removal of the oily fractions by heptane.

Figure S 5. Rheological properties at 1 Hz of a bitumen modified with TPU13. Loss factor of blends containing different TPU contents as a function of temperature.

Figure S 6. Rheological properties of bitumens modified with 15 wt% of TPU at 1 Hz. Loss factor of blends containing TPUs with different HS contents as a function of temperature.

Figure S 7. Wide angle X-ray scattering intensity of pure MDI/BDO hard segment.

Table S 1. R&B softening point of bitumen and TPU-bitumen blends containing 9, 13, and 17wt% TPU.

AUTHOR INFORMATION

Corresponding Authors

Email: gallu.raissa@gmail.com

Telephone: +33 (0)4 72 43 72 58. Email: florent.dalmas@insa-lyon.fr

ACKNOWLEDGMENT

The authors express their thanks to Soprema and Eiffage Infrastructures for their financial support, advices and help in the bitumen material characterization. The “Centre Technologique des Microstructures, plateforme de l’Université Claude Bernard Lyon 1”, CTμ and the CLYM are acknowledged for granting access to their equipment.

ABBREVIATIONS

AFM, atomic force microscopy; BDO, 1,4-butanediol; DMA, dynamic mechanical analysis; DSC, differential scanning calorimetry; HS, hard segment; MDI, 4,4'-methylene bis(phenyl isocyanate); SARA, saturates aromatics resins asphaltenes; SBS, styrene-b-butadiene-b-styrene; SEM, scanning electron microscopy; SS, soft segment; TEM, transmission electron microscopy; T_g, glass transition; TPE, thermoplastic elastomer; TPU, thermoplastic polyurethane;

REFERENCES

[1] M. Le Guern, E. Chailleux, F. Farcas, S. Dreessen, I. Mabille, Physico-chemical analysis of five hard bitumens: Identification of chemical species and molecular organization before and after artificial aging, Fuel. 89 (2010) 3330–3339. https://doi.org/10.1016/J.FUEL.2010.04.035.

[2] L. Loeber, G. Muller, J. Morel, O. Sutton, Bitumen in colloid science: a chemical, structural and rheological approach, Fuel. 77 (1998) 1443–1450. https://doi.org/http://dx.doi.org/10.1016/S0016-2361(98)00054-4.

[3] D. Lesueur, The colloidal structure of bitumen: Consequences on the rheology and on the mechanisms of bitumen modification, Adv. Colloid Interface Sci. 145 (2009) 42–82. https://doi.org/10.1016/j.cis.2008.08.011.

[4] F. Handle, J. Füssl, S. Neudl, D. Grossegger, L. Eberhardsteiner, B. Hofko, M. Hospodka, R. Blad, H. Grothe, The bitumen microstructure : A fluorescent approach, Mater. Struct. 49 (2016) 167–180. https://doi.org/10.1617/s11527-014-0484-3.

[5] J. Ancheyta, G. Centeno, F. Trejo, G. Marroquı, J.A. Garcı, E. Tenorio, A. Torres, Extraction and Characterization of Asphaltenes from Different Crude Oils and Solvents, 41 (2002) 1121–1127.

[6] P.W. Jennings, J.A. Pribanic, M.F. Raub, J.A. Smith, T.M. Mendes, Advanced high performance gel permeation chromatography methodology, 1993.

[7] M. Boduszynski, T. Szkuta-Pochopieti, Investigations on Romashkino asphaltic bitumen . 2 . Study of maltenes fractions using inverse gas-liquid chromatography, Fuel. 56 (1977) 149–152.

[8] Y. Brion, Structure colloïdale des bitumes. Relations entre composition structure - comportement, 1984.

[9] D. Stratiev, I. Shishkova, T. Tsaneva, M. Mitkova, D. Yordanov, Investigation of relations between properties of vacuum residual oils from different origin , and of their deasphalted and asphaltene fractions, Fuel. 170 (2016) 115–129. https://doi.org/10.1016/j.fuel.2015.12.038.

[10] S. Sultana, A. Bhasin, Effect of chemical composition on rheology and mechanical properties of asphalt binder, Constr. Build. Mater. 72 (2014) 293–300. https://doi.org/10.1016/j.conbuildmat.2014.09.022.

[11] D.A. Storm, R.J. Barresi, E.Y. Sheu, Rheological study of Ratawi Vacuum residue in the 298-673 K temperature range, Energy and Fuels. 9 (1995) 168–176. https://doi.org/10.1021/ef00049a025.

[12] D. Lesueur, Rhéologie des bitumes : Principes et modifications, Rhéologie. 2 (2002)

1–30.

[13] A.T. Pauli, J.F. Branthaver, Relationships between asphaltenes, Heithaus compatibility parameters, and asphalt viscosity, Pet. Sci. Technol. 16 (1998) 1125–1147. https://doi.org/10.1080/10916469808949827.

[14] M. V. Peralta-Martínez, M.E. García-Trujillo, E.M. Palacios-Lozano, G. Blass-Amador, The Effect of SARA Fractions on Viscosity for Five Mexican Vacuum Residues, Energy Sources, Part A Recover. Util. Environ. Eff. 33 (2011) 920–924. https://doi.org/10.1080/15567030903289825.

[15] P.K. Das, D. Jelagin, B. Birgisson, N. Kringos, Micro-Mechanical Investigation of Low Temperature Fatigue Cracking Behaviour of Bitumen, (n.d.).

[16] B. Isare, L. Petit, E. Bugnet, R. Vincent, L. Lapalu, P. Sautet, L. Bouteiller, The weak help the strong: Low-molar-mass organogelators harden bitumen, Langmuir. 25 (2009) 8400–8403. https://doi.org/10.1021/la804086h.

[17] S. Harders, L. Lapalu, J. Chaminaud, R. Vincent, Use of organogelator derivatives in bituminous compositions to improve the resistance of same to chemical stress, 0041075, 2013.

[18] G. Polacco, J. Stastna, D. Biondi, F. Antonelli, Z. Vlachovicova, L. Zanzotto, Rheology of asphalts modified with glycidylmethacrylate functionalized polymers, J. Colloid Interface Sci. 280 (2004) 366–373. https://doi.org/10.1016/j.jcis.2004.08.043.

[19] J. Li, W. Jia, W. Yuan, Effect of polyethylene grafted with maleic anhydride on asphalt properties, J. Perform. Constr. Facil. 28 (2014) 0401412.

https://doi.org/10.1061/(ASCE)CF.1943-5509.0000516.

[20] P.H. Yeh, Y.H. Nien, J.H. Chen, W.C. Chen, J.S. Chen, Thermal and rheological properties of maleated polypropylene modified asphalt, Polym. Eng. Sci. 45 (2005) 1152–1158. https://doi.org/10.1002/pen.20386.

[21] H. Zhang, X. Wu, D. Cao, Y. Zhang, M. He, Effect of linear low density-polyethylene grafted with maleic anhydride (LLDPE-g-MAH) on properties of high density-polyethylene / styrene – butadiene – styrene (HDPE / SBS) modified asphalt, Constr. Build. Mater. 47 (2013) 192–198. https://doi.org/10.1016/j.conbuildmat.2013.04.047.

[22] Y. Becker M, A.J. Müller, Y. Rodriguez, Use of rheological compatibility criteria to study SBS modified asphalts, J. Appl. Polym. Sci. 90 (2003) 1772–1782.

[23] C. Giavarini, P. De Filippis, M.L. Santarelli, M. Scarsella, Production of stable polypropylene-modified bitumens, Fuel. 75 (1996) 681–686. https://doi.org/10.1016/0016-2361(95)00312-6.

[24] F. Bonemazzi, C. Giavarini, Shifting the bitumen structure from sol to gel, J. Pet. Sci. Eng. 22 (1999) 17–24. https://doi.org/10.1016/S0920-4105(98)00052-7.

[25] G. Polacco, S. Filippi, F. Merusi, G. Stastna, A review of the fundamentals of polymer-modified asphalts: Asphalt/polymer interactions and principles of compatibility, Adv. Colloid Interface Sci. 224 (2015) 72–112. https://doi.org/10.1016/j.cis.2015.07.010.

[26] Y. Yildirim, Polymer modified asphalt binders, Constr. Build. Mater. 21 (2007) 66–72. https://doi.org/10.1016/j.conbuildmat.2005.07.007.

[27] N.R. Legge, Thermoplastic Elastomers, Rubber Chem. Technol. 60 (1987) 83–117.

[28] P. Redelius, Bitumen solubility model using hansen solubility parameter, Energy and Fuels. 18 (2004) 1087–1092. https://doi.org/10.1021/ef0400058.

[29] M. Liang, P. Liang, W. Fan, C. Qian, X. Xin, J. Shi, G. Nan, Thermo-rheological behavior and compatibility of modified asphalt with various styrene–butadiene structures in SBS copolymers, Mater. Des. 88 (2015) 177–185. https://doi.org/10.1016/j.matdes.2015.09.002.

[30] A. Schaur, S. Unterberger, R. Lackner, Impact of molecular structure of SBS on thermomechanical properties of polymer modi fi ed bitumen, Eur. Polym. J. 96 (2017) 256–265. https://doi.org/10.1016/j.eurpolymj.2017.09.017.

[31] J. Oliver, K.Y. Khoo, K. Waldron, The effect of SBS morphology on field performance and test results, Road Mater. Pavement Des. 13 (2012) 104–127. https://doi.org/10.1080/14680629.2011.644113.

[32] F. Dong, W. Zhao, Y. Zhang, J. Wei, W. Fan, Y. Yu, Z. Wang, Influence of SBS and asphalt on SBS dispersion and the performance of modified asphalt, Constr. Build. Mater. 62 (2014) 1–7. https://doi.org/10.1016/j.conbuildmat.2014.03.018.

[33] X. Lu, U. Isacsson, Modification of road bitumens with thermoplastic polymers, Polym. Test. 20 (2000) 77–86.

[34] A. Adedeji, T. Grunfelder, F.S. Bates, C.W. Macosko, M. Stroup-Gardiner, D.E. Newcomb, Asphalt modified by SBS triblock copolymer: Structures and properties, Polym. Eng. Sci. 36 (1996) 1707–1723.

[35] G.D. Airey, Rheological properties of styrene butadiene styrene polymer modified

road bitumens, Fuel. 82 (2003) 1709–1719. https://doi.org/10.1016/S0016-2361(03)00146-7.

[36] G.D. Airey, Viscosity-temperature effects of polymer modification as depicted by Heukelom's bitumen test data chart, Int. J. Pavement Eng. 2 (2001) 223–242. https://doi.org/10.1080/10298430108901729.

[37] G.D. Airey, Rheological evaluation of ethylene vinyl acetate polymer modified bitumen, Constr. Build. Mater. 16 (2002) 473–487.

[38] G. Polacco, S. Berlincioni, D. Biondi, J. Stastna, L. Zanzotto, Asphalt modification with different polyethylene-based polymers, Eur. Polym. J. 41 (2005) 2831–2844. https://doi.org/10.1016/j.eurpolymj.2005.05.034.

[39] M. Liang, S. Ren, W. Fan, X. Xin, J. Shi, H. Luo, Rheological property and stability of polymer modified asphalt : Effect of various vinyl-acetate structures in EVA copolymers, Constr. Build. Mater. 137 (2017) 367–380. https://doi.org/10.1016/j.conbuildmat.2017.01.123.

[40] H. Sautel, P.-E. Bindschedler, R. Perrin, Thermoplastic, elastomeric bitumen and polyurethane beads, its preparation processes and uses, Patent N°2869526, 2015.

[41] B. Bazmara, M. Tahersima, A. Behravan, Influence of thermoplastic polyurethane and synthesized polyurethane additive in performance of asphalt pavements, Constr. Build. Mater. 166 (2018) 1–11. https://doi.org/10.1016/J.CONBUILDMAT.2018.01.093.

[42] R. Yu, X. Zhu, M. Zhang, C. Fang, Investigation on the Short-Term Aging-Resistance

of Thermoplastic Polyurethane-Modified, Polymers (Basel). 10 (2018) 1–11. https://doi.org/10.3390/polym10111189.

[43] F.J. Navarro, P. Partal, M. García-Morales, F.J. Martinez-Boza, C. Gallegos, Bitumen modification with a low-molecular-weight reactive isocyanate-terminated polymer, Fuel. 86 (2007) 2291–2299. https://doi.org/10.1016/j.fuel.2007.01.023.

[44] V. Carrera, A.A. Cuadri, M. García-Morales, P. Partal, Influence of the prepolymer molecular weight and free isocyanate content on the rheology of polyurethane modified bitumens, Eur. Polym. J. 57 (2014) 151–159. https://doi.org/10.1016/j.eurpolymj.2014.05.013.

[45] A.A. Cuadri, M. García-Morales, F.J. Navarro, P. Partal, Processing of bitumens modified by a bio-oil-derived polyurethane, Fuel. 118 (2014) 83–90. https://doi.org/10.1016/j.fuel.2013.10.068.

[46] M.J. Martín-Alfonso, P. Partal, F.J. Navarro, M. García-Morales, C. Gallegos, Use of a MDI-functionalized reactive polymer for the manufacture of modified bitumen with enhanced properties for roofing applications, Eur. Polym. J. 44 (2008) 1451–1461. https://doi.org/10.1016/j.eurpolymj.2008.02.026.

[47] M.A. Izquierdo, F.J. Navarro, F.J. Martínez-Boza, C. Gallegos, Novel stable MDI isocyanate-based bituminous foams, Fuel. 90 (2011) 681–688. https://doi.org/10.1016/j.fuel.2010.10.002.

[48] B. Singh, M. Gupta, L. Kumar, Bituminous polyurethane network: Preparation, properties, and end use, J. Appl. Polym. Sci. 101 (2006) 217–226.

https://doi.org/10.1002/app.23198.

[49] R.K. Padhan, A.A. Gupta, Preparation and evaluation of waste PET derived polyurethane polymer modified bitumen through in situ polymerization reaction, Constr. Build. Mater. 158 (2018) 337–345. https://doi.org/10.1016/j.conbuildmat.2017.09.147.

[50] M.F. Sonnenschein, Polyurethanes sciences, technology, markets, and trends, Hoboken, John Wiley & Sons, Inc, New Jersey, USA, 2015.

[51] E. Delebecq, J.P. Pascault, B. Boutevin, F. Ganachaud, On the versatility of urethane/urea bonds : Reversibility, blocked isocyanate, and non-isocyanate polyurethane, Chem. Rev. 113 (2013) 80–118. https://doi.org/10.1021/cr300195n.

[52] C. Prisacariu, Polyurethane elastomers from morphology to mechanical aspects, Springer, 2011.

[53] J. Schindelin, I. Arganda-Carreras, E. Frise, V. Kaynig, M. Longair, T. Pietzsch, S. Preibisch, C. Rueden, S. Saalfeld, B. Schmid, J. Tinevez, D. White, V. Hartenstein, K. Eliceiri, P. Tomancak, A. Cardona, Fiji: an open-source platform for biological-image analysis. Nature methods 9(7), (2012) 676–682. https://doi.org/10.1038/nmeth.2019.

[54] D. Nečas, P. Klapetek, Gwyddion: An open-source software for SPM data analysis, Cent. Eur. J. Phys. 10(1) (2012) 181–188. https://doi.org/doi:https://doi.org/10.2478/s11534-011-0096-2.

[55] X. Lu, M. Langton, P. Olofsson, P. Redelius, Wax morphology in bitumen, J. Mater. Sci. 40 (2005) 1893–1900. https://doi.org/10.1007/s10853-005-1208-4.

[56] Y. Wang, K. Zhao, Different forms of asphaltene microstructures discovered in transmission electron microscopy, J. Mater. Civ. Eng. 28 (2016) 1–12. https://doi.org/10.1061/(ASCE)MT.1943-5533.0001660.

[57] G.A. Camacho-Bragado, P. Santiago, M. Marin-Almazo, M. Espinosa, E.T. Romero, J. Murgich, V. Rodriguez Lugo, M. Lozada-Cassou, M. Jose-Yacaman, Fullerenic structures derived from oil asphaltenes, Carbon N. Y. 40 (2002) 2761–2766.

[58] F. Trejo, J. Ancheyta, M.S. Rana, Structural characterization of asphaltenes obtained from hydroprocessed crude oils by SEM and TEM, Energy and Fuels. 23 (2009) 429–439.

[59] J.F. Masson, G.M. Polomark, P. Collins, Time-dependent microstructure of bitumen and its fractions by modulated differential scanning calorimetry, Energy and Fuels. 16 (2002) 470–476. https://doi.org/10.1021/ef010233r.

[60] R. Gallu, F. Méchin, F. Dalmas, J.-F. Gérard, R. Perrin, F. Loup, On the use of solubility parameters to investigate phase separation-morphology-mechanical behavior relationships in TPUs - under soumission, Polymer (Guildf). (2020).

[61] L. Cuvé, J.P. Pascault, G. Boiteux, Synthesis and properties of polyurethanes based on polyolefin : 2 . Semicrystalline segmented polyurethanes prepared under heterogeneous or homogeneous synthesis conditions, Polymer (Guildf). 33 (1992) 3957–3967.

[62] J.S. Chen, C.C. Huang, Fundamental characterization of SBS-modified asphalt mixed with sulfur, J. Appl. Polym. Sci. 103 (2007) 2817–2825.

https://doi.org/10.1002/app.24621.

[63] L. Cuvé, J.P. Pascault, G. Boiteux, G. Seytre, Synthesis and properties of polyurethanes based on polyolefine : 1 . Rigid polyurethanes and amorphous segmented polyurethanes prepared in polar solvents under homogeneous conditions, Polymer (Guildf). 32 (1991) 343–352.

[64] E. Saroufim, C. Celauro, M.C. Mistretta, A simple interpretation of the effect of the polymer type on the properties of PMBs for road paving applications, Constr. Build. Mater. 158 (2018) 114–123. https://doi.org/10.1016/J.CONBUILDMAT.2017.10.034.

[65] M. Takayanagi, S. Uemura, S. Minami, Application of equivalent model method to dynamic rheo-optical properties of crystalline polymer, J. Polym. Sci. Part C Polym. Symp. 5 (1964) 113–122. https://doi.org/10.1002/polc.5070050111.

[66] N. Ouali, J.Y. Cavaille, J. Perez, Elastic, viscoelastic and plastic behavior of multiphase polymer blends, Plast. Rubber Compos. Process. Appl. 16 (1991) 55–60.

[67] J. Kolarik, Simultaneous prediction of the modulus, tensile strength and gas permeability of binary polymer blends, Eur. Polym. J. 34 (1998) 585–590. https://doi.org/10.1016/S0014-3057(97)00176-6.

[68] P.G. De Gennes, On a relation between percolation theory and the elasticity of gels, J. Phys. Lett. Paris. 37 (1976) 2. https://doi.org/DOI: 10.1051/jphyslet:019760037010100.

[69] L.H. Sperling, Introduction to physical polymer science, John Wiley & Sons, 2005.

SUPPORTING INFORMATION

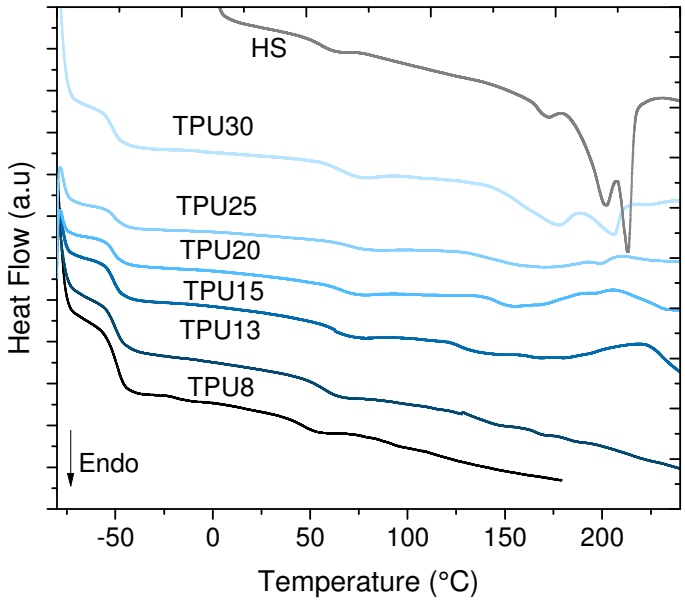

Figure S 1. Differential scanning calorimetry traces of TPU having various MDI/BDO hard segment contents and of the pure MDI/BDO hard segment

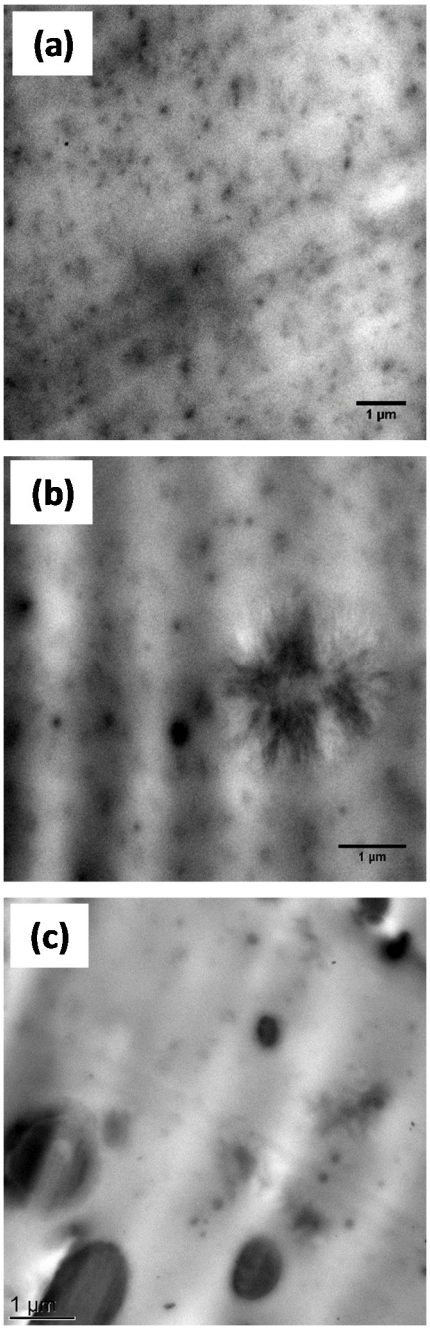

Figure S 2. TEM images of TPU containing MDI/BDO hard segments: a) 13wt% HS; b) 15wt% HS; c) 30wt% HS.

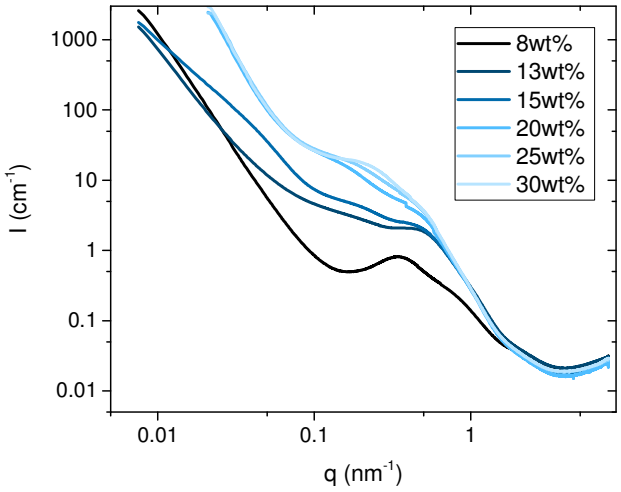

Figure S 3. SAXS patterns of TPU varying from their HS content.

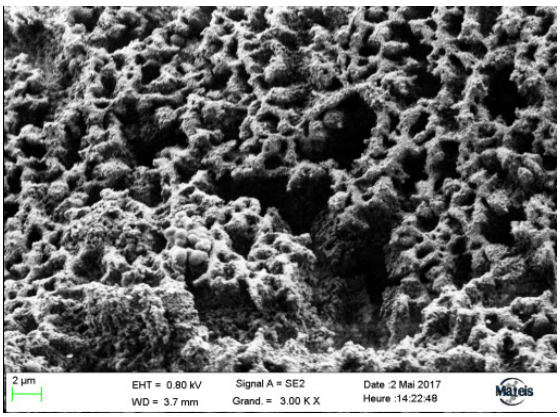

Figure S 4. SEM image of blend containing 17wt% TPU13 after removal of the oily fractions by heptane.

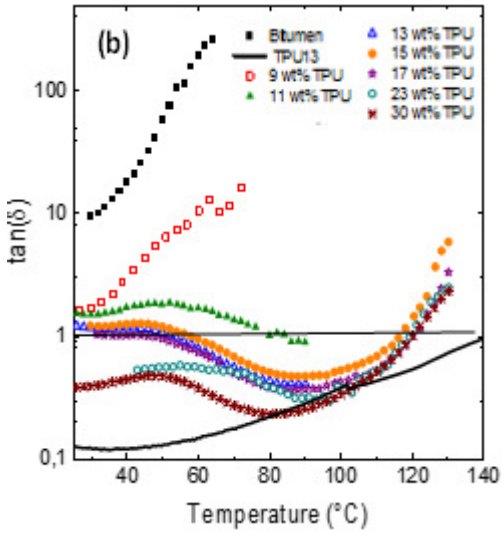

Figure S 5. Rheological properties at 1 Hz of a bitumen modified with TPU13. Loss factor of blends containing different TPU contents as a function of temperature.

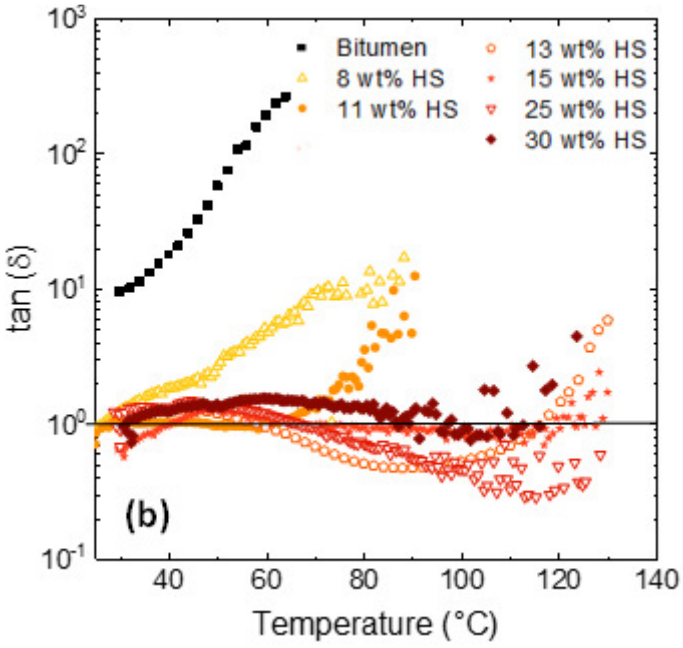

Figure S 6. Rheological properties of bitumens modified with 15 wt% of TPU at 1 Hz. Loss factor of blends containing TPUs with different HS contents as a function of temperature.

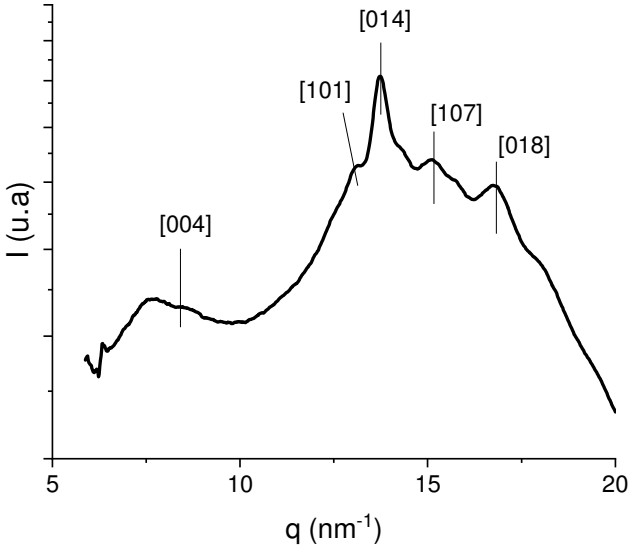

Figure S 7. Wide angle X-ray scattering intensity of pure MDI/BDO hard segment.

Table S 1. R&B softening point of bitumen and TPU-bitumen blends containing 9, 13, and 17wt% TPU.

	Bitumen	9wt%	13wt%	17wt%
R&B softening point (°C)	43	49	109	113